Robust CAD Methodology for CFD optimizations

Patrick Wegener⋆
⋆*German Aerospace Center (DLR)*
Lilienthalplatz 7, 30108 Braunschweig, Germany
patrick.wegener@dlr.de

Abstract

Automatically updated CAD models are the foundation for a CFD-based optimization. Since any interruption of the geometry update will falsify the result, a robust model is a prerequisite. Using the DLR-F25 configuration as an example, the methodology as a basis for a robust model is described by components, both in terms of the structure of the models and the hierarchical setup of the CAD features. The robustness is addressed in terms of causes and solutions, and an automated update analysis method is described. Since the CAD model is required at the beginning of the CFD process chain, its influence on the result is fundamental. Therefore, an accurate CAD setup is the basis for a successful CFD simulation.

1. Introduction

The field of Computer Aided Design (CAD) covers an extensive range of applications. This paper focuses on the subject of the generation of surface data of commercial aircraft as a basis for shape optimization, in the course of which no manual intervention is intended anymore. Thus, CAD modeling can be compared to a "geometrically modeled" algorithm, which transforms the input parameters into unique surface data. For this purpose, the software CATIA from Dassault Systèmes was used. Since the procedure is described in general terms, it should be applicable to a large number of parametric-associative CAD systems. *Parametric* in this case means that - in contrast to static data formats such as the IGS or STEP - geometries can be modified by changing input parameters and then updating them, while *associativity* describes the linking of parameters to each other in the form of a mathematical graph: an update thus triggers a cascade of update processes. Usually, no redundancy is provided in such a system, which is why any error leads to an abort of the geometry update. This relation is especially relevant in the context of a multi-parameter optimization, since its results can be biased by such CAD update aborts.

The topic of CAD for robust CFD models is described differently in literature: at an abstract level, reuse and standardization using knowledge-based engineering (KBE) is addressed by Verhagen [1]. In contrast, the work of Agarwal et al describe in great detail the modeling of abstract surface elements for the purpose of advanced optimization methods [2]. The preliminary design is addressed in the work of Haimes [3] and Liersch [4]. For this purpose, they use reduced CAD systems, which are not widely used in the commercial sector. With regard to CATIA as a widespread standard in the aerospace industry, concrete basic literature can be found on the one hand [5], and on the other hand more high-level documentation, such as for the structured, company-internal use [6]. On a level of detail in between these extremes, the present work is intended to continue the work of Ronzheimer [7] in order to go more into detail and to address robustness as well - a topic that is otherwise described on a rather abstract level [8].

Since the methodological structure has a significant influence on the robustness of a CAD model, the first part of the paper deals with this topic, before the second part explains the causes and possible solutions of CAD robustness. As part of the "VirEnfREI" project - funded by the German LuFo programme - a small/medium range configuration of high aspect ratio is being investigated, which will be used as DLR-F25 reference configuration in numerous parallel projects. For this reason, the methodical construction of robust CAD geometries will be explained on the basis of this geometry.

2. Methodology

In a "geometrically modeled" algorithm - especially in the context of MDO investigations - a complex set of numerous, multiply curved surfaces is described as a result by hundreds of input parameters. The methodology provides the comprehensible and explicit connection between them. The term methodology is divided here into *structure* and *setup*. The structure is used exclusively for human readability: since the associativity is given in the definition of the
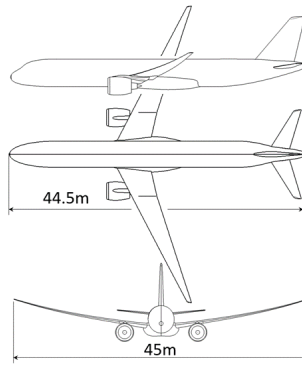
ROBUST CAD FOR CFD

Figure 1: 3-View of the DLR-F25 Configuration

graph, the structure of the CAD model is irrelevant for the update process. However, analogous to source code in the software domain, the quality of the structure influences the traceability, debugging as well as the reuse of the partial models in alternative contexts. When it comes to setup, there is no single best approach. Rather, there is a spectrum of options that make varying degrees of sense. Basically, in the CAD context, the clear assignment of the complex shaped geometries to simple parameters should be achieved (e.g. aspect ratio of the wing), while all others (e.g. wing twist) remain uninfluenced by it. At the same time, the "curse of dimensionality" should be avoided especially in the context of optimization: The shape of a wing airfoil curve, for example, should be described with as small a number of parameters as possible, but at the same time larger changes in curvature should remain possible. Ideally, a state is achieved which always results in a reasonable geometry even with a random selection of parameters.

2.1 Structure

The geometry of the F25 is divided into several files, which are based on comparable basic concepts:

- IPO model: In the feature tree, input/processing/output is structured vertically below each other. This also applies to the substructures, so that the top element represents the beginning of the substructure, and the bottom element always represents the (partial) result.

- Reference structures are geometries that are informally contained in the model as a template or for comparison. These are also arranged at the top of the structure tree. This area is the only one that may contain isolated non-parametric geometries. These are not integrated into the parametric structure.

- The structuring of the feature containers ("Geometrical Sets" in CATIA) are based on a hierarchical structure and are named accordingly - comparable to comments in source code.

- Parameters are divided into primary and secondary ones: Primary parameters are explicitly highlighted as CATIA parameters. The secondary parameters derived from them are arranged within the feature tree (Fig.2). Manual changes to scalar input variables are therefore only made to the primary parameters, while the actual feature tree follows the automatic update.
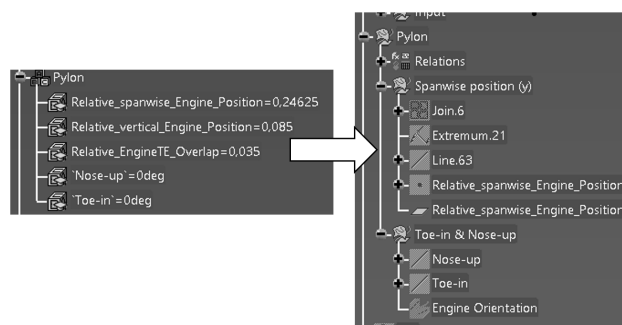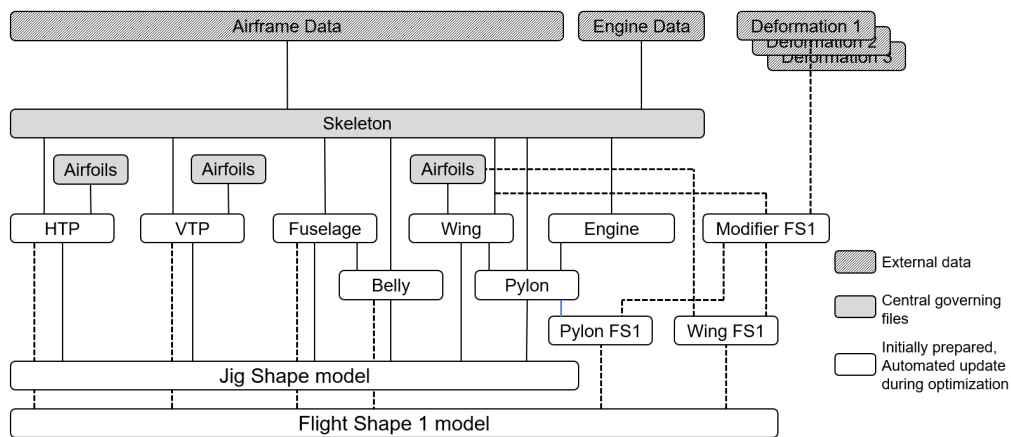

Figure 2: Primary and secondary parameters

Figure 3: External file hierarchy

The linking of the files to each other is similarly structured (Fig.3): A superordinate skeleton model forms the basis of the entire configuration. All input parameters are collected, prepared and made available as published links to the other files. Design tables of ASCII text files form the external link of the model. They contain only one line, the current parameter values. During optimisation, these files are modified by external scripts, and the models are updated subsequently. Parallel to the skeleton model, the wing airfoil curves are defined in individual parts. This allows simple variation or replacement of the mathematical representation (e.g. CST instead of Bézier formulation) independent of the rest of the aircraft parametrics. It also allows the same profile to be used multiple times without creating redundancy. The linked parts are further differentiated hierarchically: primary parts (e.g. wings, HTP) are directly linked to the skeleton, while the secondary parts additionally require the primary ones as input. For example, the pylon uses the engine and wing as input geometry, while the position and orientation of the engine is defined in the skeleton model. Finally, the positioned surface data of all components are collected in a separate model, mutually trimmed and merged into connected subdomains (e.g. wing upper side, wing lower side, fuselage). In addition, geometric elements are defined for local mesh refinement (see chapter 2.5). This process occurs multiple times: the undeformed initial geometry is generated in the jigshape model, while the elastic deformation is considered in respective flightshape models.

2.2 Setup

The modelling of each component is described below. Bézier curves are often used to create the surfaces, so their CATIA modelling is briefly described: In the CATIA Workbench "Generative Shape Design (GSD)" the spline function is available for curve generation. This function can be used to define curves that pass exactly through the underlying points - depending on the quality of the coordinates, this may result in a wavy curve. Unlike the parametric GSD Workbench, the "Freestyle Shaper" Workbench allows direct manipulation of control points, but usually not parametrically. An exception is the "3D Curve" function, which can be used to create a parametric link to control points.
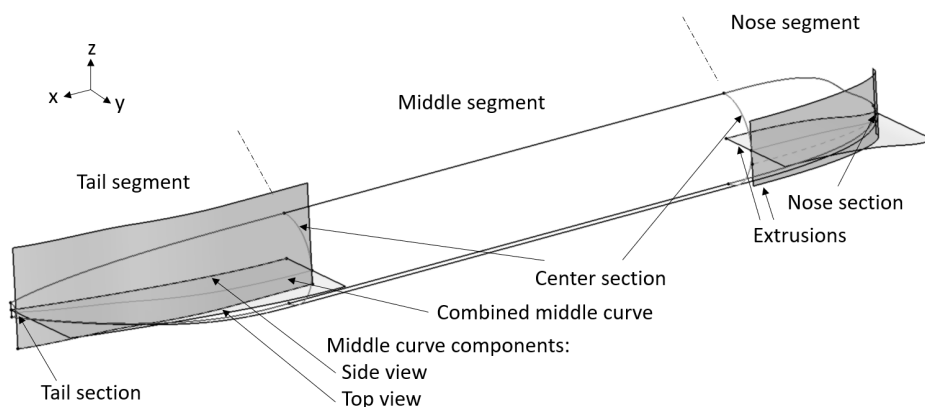

Figure 4: Fuselage surface, section and guide curves

ROBUST CAD FOR CFD

2.2.1 Fuselage

The fuselage consists of three segments (Figure 4) : nose, prismatic middle and tail section. Of the section curves, the center section is the central element of the fuselage: it forms the end of the nose segment, the base of the extrusion surface for the center, and the beginning of the tail segment. It is complemented by the nose section, which forms the start of the front segment, and the tail section, which forms the end.

To span the Multi Section Surfaces in between, three guide curves each are used in the front and rear segments. The upper and lower guide curves on the symmetry plane zx are realized by planar Bézier curves, while the modeling of the middle curve is split into two component curves: A curve on the zx-plane forms the side view of the curve, while a curve on the xy-plane describes the top view. An extrusion of both curves followed by an intersection results in the three-dimensional middle guide curve. In this way, both the cockpit area can be harmonically designed, as well as the flattened area of the later intersection with the horizontal stabilizer. This technique is used multiple times in the further course of the design to model three-dimensional guide curves.

2.2.2 Wings

In this paper, wings are all surfaces which - in contrast to the fuselage - can specifically generate lift, i.e. also the tailplane and rudder. In terms of construction, they are identical:

Wing airfoils   Numerous methods for modeling airfoils are described in the literature [9], [10]. In the VirEnfREI project, a simple approach using Bézier curves was followed. To determine the best tradeoff between the number of control points on the one hand and the ability to resolve local curvature changes on the other, the approach of parameterizing a small number of control points in x and y position was discarded.
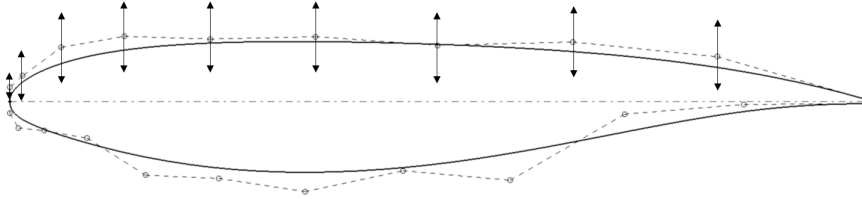

Figure 5: Overview of the Airfoil Bézier curves, similar variation of the lower side control points

Instead, more control points are used whose x coordinates are defined by a cosine distribution. In the course of optimization, only their vertical coordinate is varied (Figure 5). On the top side, a 9th order curve has been found to be useful, while the bottom side is described by an 11th order curve.

The transition between the two curves is calculated using a formal relationship. The curvature of Bézier curves in general [11] is defined via (1) :

$$\kappa(t) = \frac{|\dot{x}(t) \times \ddot{x}(t)|}{|\dot{x}(t)|^3} \tag{1}$$

For the special case of the beginning ($t = 0$) this simplifies to (2).

$$\kappa(0) = \frac{\left| n \cdot \Delta a_0 \times n \cdot (n-1) \cdot \Delta^2 a_0 \right|}{|n\Delta a_0|^3} \tag{2}$$

This can be reformulated to (3):

$$\kappa(0) = \frac{(n-1) \cdot 2 \cdot A_{X_0 U_1 U_2}}{n \left| \overline{X_0 U_1} \right|^3} \tag{3}$$

It can be seen that the curvature is determined, in addition to the degree n of the Bézier curve, only by the area A_1 defined by the points X_O, U_1 and U_2 and the distance between X_0 and U_1. Since the curvature of the top and bottom of the profile must have the same value at the nose, this formula can be equated and resolved to the distance l (Figure 6):

$$l = \sqrt{\frac{h}{2 \frac{(n_1-1)n_2 A_1}{(n_2-1)n_1 u^3}}} \tag{4}$$

This equation is defined in CAD as a formula for the definition of the coordinate l, so that a constant curvature transition is maintained in all cases.
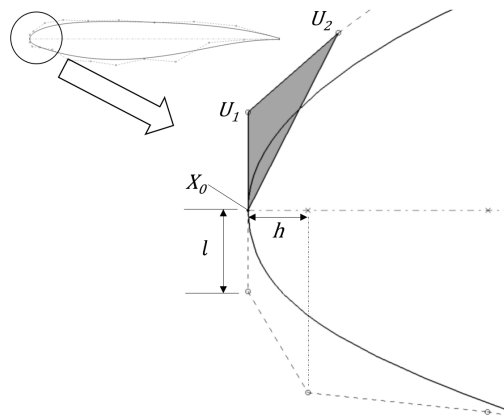
Figure 6: Detail of the airfoil nose control points

Guide curves In addition to the airfoils, leading and trailing edge guide curves are required to build up the wing surfaces. These depend on the spanwise distribution of Sweep, Dihedral, Twist and Chord.

Along the span, these variables are each described as a curve in order to build up the leading curves in a multi-step procedure: The dihedral and sweep curves are defined on the orthogonal yz and xy planes, respectively, and assembled by extrusion and intersection - analogously to the center fuselage guide curves. This "wing spine" later runs between the leading and trailing edge of the wing, in this case at 25% of the wing chord (Figure 7):
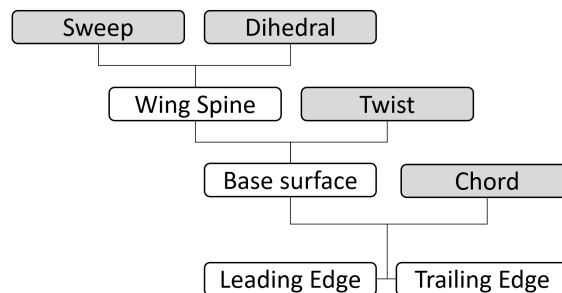

Figure 7: Hierarchy of the guide curves

The CATIA "Generative shape design" Workbench contains the "Law" function. This offers the possibility to establish formal relationships between a reference curve - here a straight line in y-direction along the half-span - and a further curve. In this process, it is possible to convert units. In the case of wing twist, one meter of vertical distance from the reference curve corresponds to one degree of twist.

The twist curve is defined at 6 characteristic y-coordinates, through which a spline curve is formed - the definition curve of the Twist Law. With this and the curve of the wing spine, the twisted "base surface" of the wing is modeled, on which the leading and trailing edges are located. From the scalar planform parameters wing area, aspect ratio, taper, position and chord of the wing sections, the projected wing planform is formed in the form of a sketch on the xy plane. Since the projected wing surface should remain independent of the twist course, the leading and trailing edges of the wing are formed by a vertical projection of the planform onto the base surface (Figure 9).
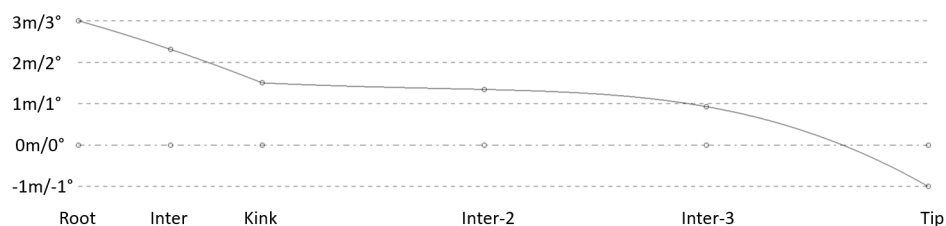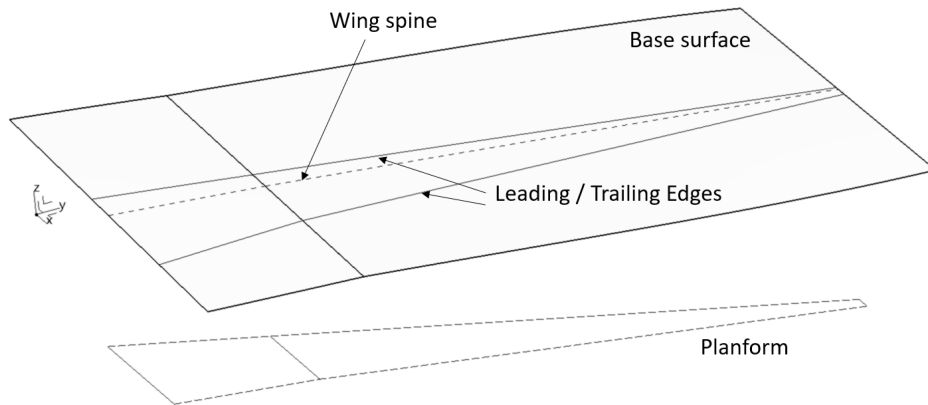

Figure 8: Spline curve defining the twist law

Figure 9: Wing Guide Curves

Surfaces   The wing airfoils are scaled, positioned and oriented normal to the dihedral curve. The short curves of the profile trailing edges serve as section curves from which the surface of the blunt trailing edge is formed along the trailing edge. Their upper and lower edge curves - together with the leading edge - then form the guide curves for the wing basic surfaces. For aerodynamic reasons, the configuration is given a rounded wingtip. Mathematically, a Gordon surface always has four edges. If one wanted to design the rounded wingtip by connecting a surface directly to the boundary of the wing surface, that surface would only have three edges. To avoid this situation, the wing base surface is trimmed and the wing tip surface is added (Figure 10).
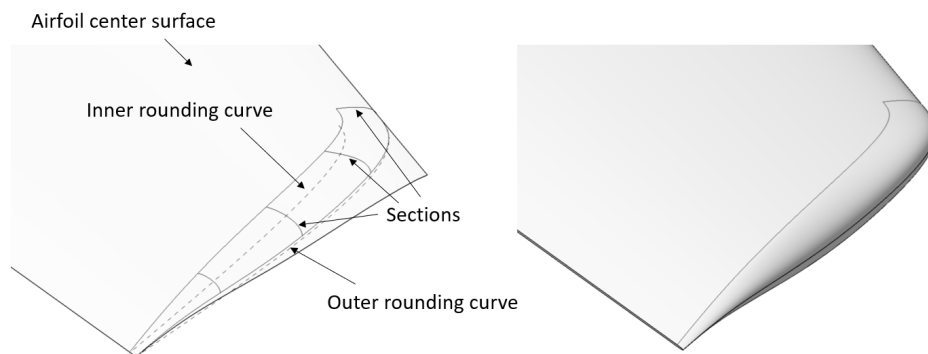

Figure 10: Design and result of the rounded wingtip

The wingtip is composed of an upper and a lower surface, each of which is defined by sections and guide curves, and a tangential boundary condition normal to the wing base surface. The leading curves are defined by an outer and an inner rounding curve, which are then projected: in the case of the inner curve, onto the upper and lower wing planform surfaces, respectively; in the case of the leading curve, onto the airfoil center surface spanned by the skeleton curves of the airfoils The sections are formed by curves on planes perpendicular to the outer rounding curve, which intersect the wing basic surfaces in the case of the first curve and enter it tangentially at the end in the case of the others. The last section is a conic curve that rounds the trailing edge surface in a D-shape.

2.2.3   Engine

Engine and pylon are built sequentially: Based on the dimensions given from the skeleton model, the engine surfaces are modeled, which are attached to the wing in the second step. In the case of the DLR-F25, information on fan and core dimensions and their outlet surface areas form the primary parameters of the engine nacelle. The secondary parameters are modeled according to a reference nacelle and linearly scaled to the primary parameters. The engine is built up at the CAD coordinate origin from the inside to the outside (Figure 11):

Inner surfaces   Based on the inner coordinates of the fan intake, the spinner curve is formed. On the output side, the inner coordinate of the core outlet determines the start of the plug curve, the length of which is scaled by the core
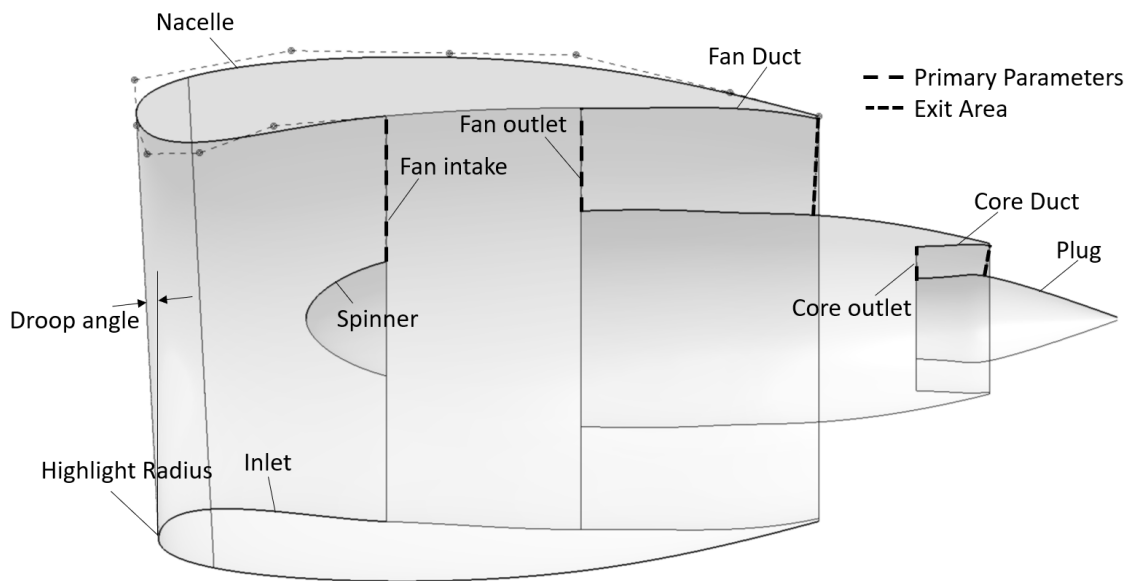
Figure 11: Guide curves of the DLR-F25 engine design

diameter. Based on this, the course of the cross-section area of the core channel determines its outer side, the core duct. The bypass duct is also built from the inside out: Starting from the inner coordinate of the fan outlet, the core cowling runs to the end of the core duct. Again, its outer side, the fan duct, is determined by the course of the area of the bypass cross section. Together with the trailing edge thickness of the nacelle, the end point of the nacelle is determined. The inner surfaces are formed by rotating these curves around the engine axis.

Inlet and Nacelle   The nacelle outer surfaces are designed as multi-section surfaces based on the section curves of the outer side, as well as the highlight radius and the nacelle trailing edge as guide curves. Both guide curves are circular. An asymmetry results from the highlight radius being tilted around the droop angle. The inlet surfaces are designed analogously, with the highlight radius as the leading and the fan outer diameter as rear guide curve. Mathematically, the nacelle section curves are modeled as 6th order Bézier curves, with the last 4 control points of the bottom of the nacelle generated by mirroring the top control points, while the first three coordinates are determined via an intersection with the highlight curve and adjusted linear factors. The curves of the inlet are also generated as Bézier curves, here the curvature continuous transition is ensured analogous to the wing profiles by a formal relation as described in (4).

2.2.4 Pylon

The aim of pylon modelling - in addition to aerodynamic accuracy and watertight CAD robustness - is to generate geometries that do not trigger shock-induced separations over a wide range of parameters. This requires the use of relative angles and distances, since absolute values generate results in spatial displacements that already appear visually strange and induce flow separation.
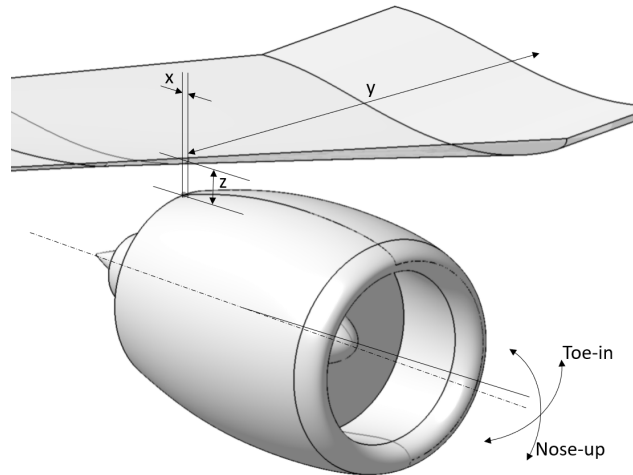

Figure 12: Engine position and orientation

Engine positioning   The wing lower surface, engine surfaces, and alignment information are used to model the pylon. In the first step, the positioning of the engine trailing edge relative to the wing leading edge as well as the rotations around y and z axis are performed on this basis (Figure 12). Subsequently, the pylon surfaces are modelled to cover the engine-wing joint:

Pylon Surfaces   The pylon modeling starts with the definition of the side surfaces of the pylon. For this purpose, a center surface is first built up, which runs through an upper and lower reference curve. The lower reference curve is formed by the engine axis. The upper reference curve is built up in two parts: Below the wing, it is defined by the "pylon yaw", a rotation around the z-axis. In the area of the engine, this runs parallel to the toe-in angle of the engine. A transition area ensures the smooth curve shape (Figure 13).
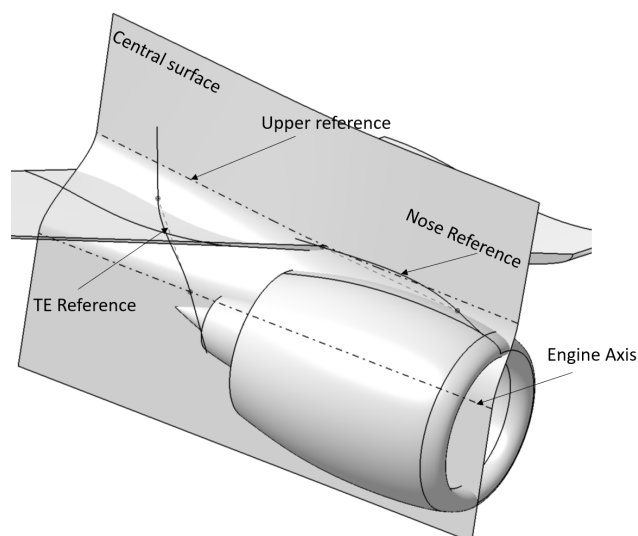

Figure 13: Pylon base geometries

The course of the trailing edge and nose curve is defined by relative angles: For this purpose, a reference line is defined in each case, to which constant angles are specified at both ends - the later end tangents of the curves. On the wing side, the end points of the reference line are defined by relative chord positions; on the engine side, the trailing edge point is defined as the distance from the core trailing edge, and the nose point is defined by a relative chord ratio of the upper nacelle airfoil. The section curves to build up the pylon sidewalls are defined by an airfoil with the pylon width open at the front. This is used translationally displaced in the wing and engine side sections. The inner side is defined by a symmetry of the pylon airfoil at the center surface. Together with the pylon trailing edge, this results in the pylon side surfaces.
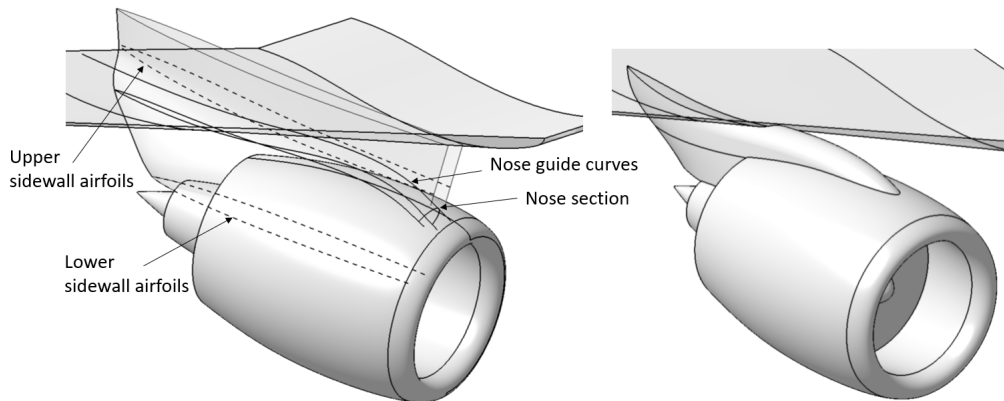

Figure 14: Pylon base geometries and final geometry

The front end of the pylon is formed by the nose surface, which runs through three guide curves: the middle guide curve is formed by the projection of the nose curve onto the center surface, the outer ones are formed by a parallel shift of the projections of this guide curve on the side surfaces. A simple spline forms the section curve of the nose surface. The total watertight volume is then formed via multiple trim operations.

2.3 Belly Fairing

Due to the high aspect ratio of the DLR-F25 configuration, the landing gear no longer fits in the wing, which is why a body-mounted landing gear is used. The dimensions of the belly fairing are therefore based on simplified landing gear kinematics in addition to the fuselage and wing. The belly fairing is again built as a multi-section surface based on Bézier curves. Since the surface finally intersects with the fuselage and wing surfaces, no tangent continuities have to be taken into account for the design of the curves.
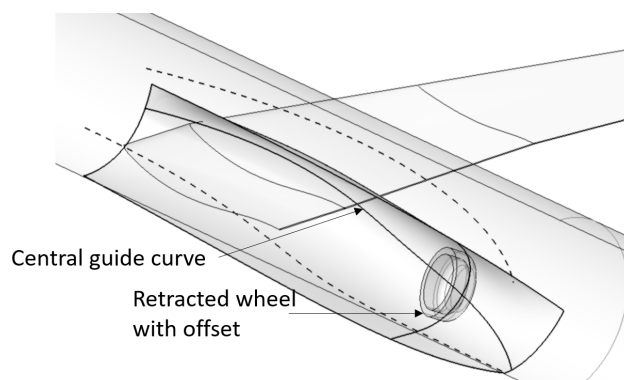

Figure 15: Belly fairing design basics

For the center section curve, an offset surface of the outer wheel finds its way into the design (Figure 15), while the front and rear curves are shaped relative to the fuselage contour.The front fairing length is defined by a distance relative to the root chord length, while the rear extension is dimensioned by a distance relative to the wheel center. The upper guide curve depends on the fuselage contour, while the position of the wheel influences the course of the lower guide curve. Since the landing gear causes a large extension slightly below the wing when retracted, a central guide curve

composed of two curves is used here again. This allows a harmonious transition from the wing over the necessary landing gear clearance into the fuselage contour.

2.4 Aeroelastic wing deformation

In the Virenfrei project, it should be possible to investigate large geometric changes during optimization. Furthermore - due to the high aspect ratio - large amplitudes are to be assumed in the area of the elastic wing deformation. To ensure these geometric degrees of freedom, the CFD mesh is generated via an automated mesh re-generation process. Therefore, the undeformed (Jigshape) geometry is modeled and adapted by optimization. From this, flight situation-dependent elastically deformed (Flightshape) geometries are derived. The CATIA internal tool "Wrap Surface" is used to model these deformations. With this tool, deformations can be performed, which are defined based on the relative position between a source and target surface. This procedure could be validated in the framework of the Drag Prediction Workshop No. 7 [12]. In the Virenfrei project, the aeroelastic deformations of the rib centers are provided by members of the consortium, so that translational and rotational deformations are defined at 31 spanwise positions. During the MDO optimization process, these deformations are iteratively modified. In order to have at least an approximate deformation in case of a geometric wing change, the coordinates are first linearly interpolated from the wing planform on which the structural simulation is based to the current wing planform.
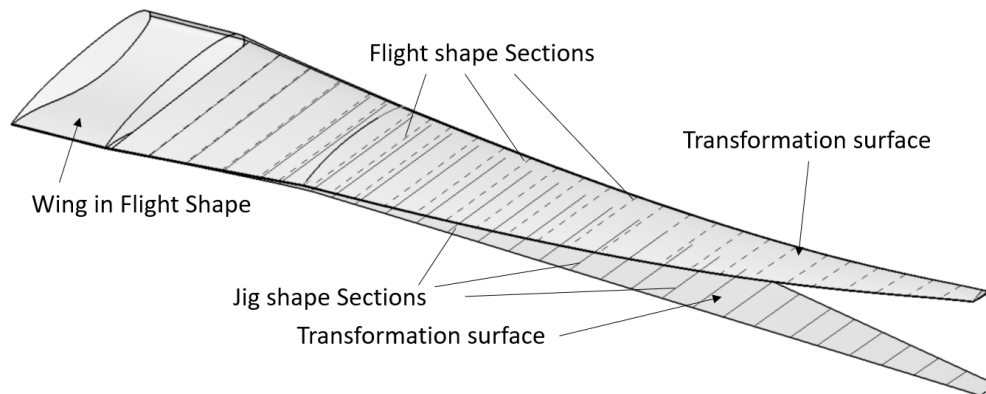

Figure 16: Elastic Wing deformation

Subsequently, lines of local wing chord and twist angle were generated at both the current and deformed 31 positions (Figure 16). Both sets of curves were then used to model the source and target surfaces. To avoid distortion of the airfoils, vertical deformation of the airfoil sections should be avoided. Furthermore, the circular cross-section of the inner elements of the engine should remain unchanged. Therefore, only the leading and trailing edges and the positions of the wing sections were deformed. The Flightshape wings were then remodeled in the same way as the Jigshape geometry using the identical airfoil curves. A pair of axis systems was defined to reposition the engine and pylon. Multiple trim operations are then used together with the tailplane and fuselage geometries to create the entire aircraft in the appropriate flight configuration.

2.5 Adaptive meshing sources

The final phase is the creation of the auxiliary geometries for the CFD simulation: on the one hand this is the far-field box with several spans distance around the aircraft, on the other hand these are local refinement sources: The used mesh generation software "Centaur" offers the possibility to define regions of local mesh refinement using auxiliary geometries defined by coordinates such as frustums, hexahedrons and tubes.
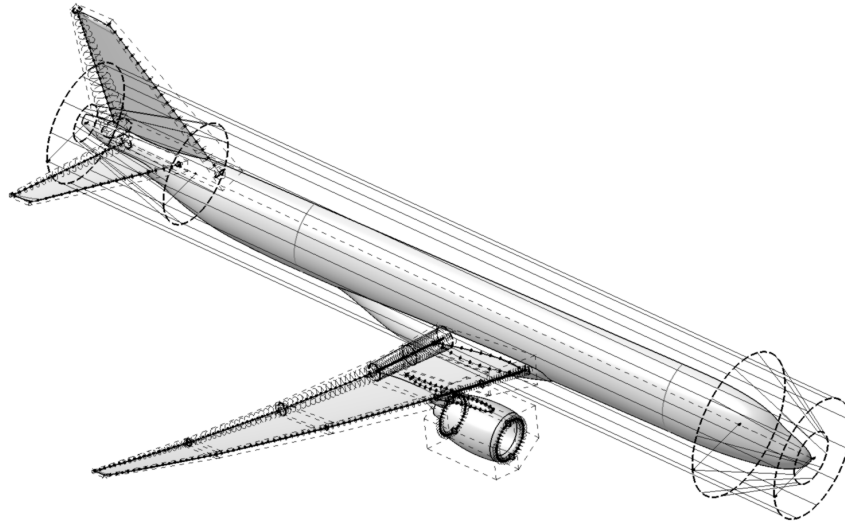
Figure 17: Final CFD Geometry with local refinement sources

These are defined and visualized in the model (Figure 17), their numerical information is finally transferred from CAD to Centaur format via scripts [7]. The local refinement of the wing trailing edge thus always follows its geometric adaptations in the course of optimization as well as the elastic deformations.

3. Robustness

Due to the hierarchical structure of the parametric CAD model, a single update failure leads to its termination. In the following, their causes will be analyzed and possible stabilization measures will be presented.

3.1 General

CAD instabilities are highly dependent on the CAD system used. Furthermore, errors are often not caused by a single parameter, but only occur with certain parameter combinations. Therefore, the robustness of the CAD model should be validated before optimization. For a detailed analysis and an increase of robustness, a procedure as described in figure 18 is recommended: CATIA offers the possibility to store parameter combinations in the form of design tables. In a first step, such tables are filled with randomly generated values of the parameter space, in order to perform automatically logged update attempts on this basis. In the second step, the failed attempts are selected successively and their failure cause is eliminated. Iterative execution can effectively reduce the number of aborts and thus increase robustness. Since fixing CAD aborts is easier said than done, the causes and possible solutions will be discussed in the following.

3.2 Boundary Representations

When creating boundary operations, points, edges or faces of neighboring geometries often serve as input data for subsequent operations. A change in the spatial position of these elements - due to a change in the initial parameters - can lead to an incorrect reassignment. In the usual CAD process such elements are determined by their selection in space. In CATIA, internal rules are defined to reassign these edges after a change. These internal rules are the cause of instabilities, especially with larger spatial changes. In the following recommendations for the stabilization of boundary representations are given. In general, it should be avoided to select elements in CAD space, a selection directly in the feature tree being preferable, since this completely avoids the associativity of features via boundary representations. As this is not always possible, additional methods become necessary: the use of spatial location provides a very stable
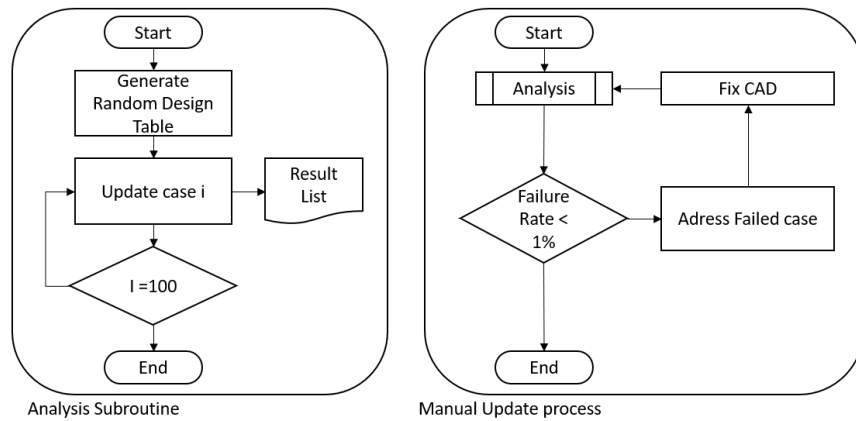
Figure 18: Flowchart of the process for robustness enhancement

way to address elements. Using the example of the selection of a single edge of a surface, the complete boundary curve of the surface is determined in the first step. In the second step, its corner points are subsequently identified via an extreme value determination. In particular, separately defined directions that deviate from the three standard vectors allow exact addressing in most cases. If edges of the surface are needed for the subsequent operations, the splitting of the boundary curve with the help of such points represents a stable assignment. In the use of the parent elements there is an additional method for the determination of edges: if, for example, the boundary curve of a split operation is searched for, it can be generated parallel to it by intersection of the involved surfaces. When selecting surfaces - for example partial surfaces of surface joins - it is more stable to rebuild individual partial surfaces analogously instead of extracting partial surfaces from a surface join.

3.3 Geometric impossibilities

Another cause of CAD instabilities are mathematical impossibilities. These are also mostly caused by unsuitable parameter combinations: If, for example, the upper side of an airfoil is described by a Bézier curve, the curve of the upper side of the airfoil can penetrate the curve of the lower side due to certain configurations of the control points. The solution approach here is more complex; besides a reduction of the parameter space, a definition of the control points relative to the neighboring points would be conceivable. Another alternative would be to define the upper side of the airfoil relative to the lower side or to define the profile using drop and camber curve. Failing split operations also belong to this group of instabilities: In general, it is not advisable to intersect surfaces at curves. The more stable method is to extend the involved surfaces accordingly to always ensure a safe penetration.

3.4 Normal alignments

Every CAD curve and surface has an orientation, which is used to define e.g. the positioning of a point on the curve or the direction of an offset. Within a parameter space, a spontaneous inversion of such orientations can occur in CATIA, which causes the subsequent operations to fail. With the near/far operation, the single element with the smallest or largest distance to a reference element can be selected from a set of several spatially separated elements in CATIA. This can be used, for example, to stabilize an offset operation that is oriented to the normal orientation: Both offset possibilities are generated, combined in an surface join, which references a spatially fixed element via the near/far operation. Another option for stabilization can be found in the CATIA Workbench "Knowledge Advisor": there are rule-based options available to model "if/then" relationships. If these are applied to elements that are affected by changing normal alignments, the reasonable subsequent operation can be determined.

3.5 Trim operations

The "Trim" functions in CATIA are convenient as they allow multiple intersections to be defined at once. Unfortunately, as the number of sub-surfaces increases, stability decreases significantly. It is therefore better to define each sub-surface using individual split operations and then merge them into a composite surface. It is also important to ensure that the intersected surfaces are sufficiently long, and to dimension the parameter space to ensure that both surface composites penetrate each other completely.

4. Outlook

In the next few years, the introduction of networked CAD databases will add new capabilities to the current modeling process. At present, the communication of the current status of the geometry is a challenge in the MDO process. Networked, cloud-based systems provide the ability to access identical data sets across company boundaries. In addition, modern systems offer the ability to parametrically link even different CAD systems so that preferred systems can be maintained. This raises questions about the limits of intellectual property protection. One approach in CATIA is the use of "user defined features". This is a method of encapsulating individual CAD steps as a separate, non-modifiable feature in the feature tree, for example components such as wings or HTP. In this way, it is possible to exchange models that can be updated without having to have full access to the detailed design. This can also be used to standardize recurring elements, speeding up the creation of initial models when investigating similar challenges, as well as the use of standardized secondary tools for analysis. However, such models can only represent existing geometries, so there still remains a strong demand for the art of CAD modeling.

5. Summary

In this paper, insight into the structure of the CAD model of the DLR-F25 was provided to describe the CAD methodology, both macroscopically in the form of a description of the linkage and structure of the files used and in detail by describing the modeling of individual components. Furthermore, the influencing factors of the CAD robustness were described exemplarily on the basis of causes and solution approaches. Since CAD instabilities are rarely caused by a single parameter, an analysis based on automated, multiple updates is strongly recommended. In publications on aerodynamic simulation of various geometries, a properly operating CAD model is usually taken for granted, but rarely described. This is deceptive in the sense that this phase is at the very beginning of the investigation and therefore has the greatest impact on the overall result. Furthermore, the time required to create a working CAD model is usually massively underestimated. Good results can only be achieved with an accurate model. The key factor is the stability of the CAD, which must always extend beyond the parameter space investigated in the optimisation.

6. Acknowledgments

References

[1] Wim J.C. Verhagen et al. "A critical review of Knowledge-Based Engineering: An identification of research challenges". In: *Advanced Engineering Informatics* 26.1 (2012), pp. 5–15. DOI: `https://doi.org/10.1016/j.aei.2011.06.004`.

[2] Dheeraj Agarwal, Simão Marques, and Trevor Robinson. "Aerodynamic Shape Optimisation Using Parametric CAD and Discrete Adjoint". In: *Aerospace* 9 (Nov. 2022), p. 743. DOI: `10.3390/aerospace9120743`.

[3] Robert Haimes and Mark Drela. "On The Construction of Aircraft Conceptual Geometry for High-Fidelity Analysis and Design". In: *50th AIAA Aerospace Sciences Meeting including the New Horizons Forum and Aerospace Exposition*. DOI: `10.2514/6.2012-683`.

[4] Carsten Liersch and Martin Hepperle. "A distributed toolbox for multidisciplinary preliminary aircraft design". In: *CEAS Aeronautical Journal* 2 (Dec. 2011). DOI: `10.1007/s13272-011-0024-6`.

[5] Maik Hertha. *CATIA V5: Flächenmodellierung*. Hanser, 2009.

[6] Siddhartho Banerjee, Percey Thomas, and Xiao Cai. "CATIA V5-Based Parametric Aircraft Geometry Modeler". In: *SAE International Journal of Aerospace* 6 (July 2013), pp. 311–321. DOI: `10.4271/2013-01-2321`.

[7] Arno Ronzheimer. "CAD in Aerodynamic Aircraft Design". In: *Deutscher Luft- und Raumfahrtkongress*. Munich, Sept. 2017.

[8] Kristian Amadori et al. "Flexible and robust CAD models for design automation". In: *Advanced Engineering Informatics* 26 (Apr. 2012). DOI: `10.1016/j.aei.2012.01.004`.

[9] Brenda M Kulfan. "Universal parametric geometry representation method". In: *Journal of aircraft* 45.1 (2008), pp. 142–158.

[10] D. A. Masters et al. "Geometric Comparison of Aerofoil Shape Parameterization Methods". In: *AIAA Journal* 55.5 (2017), pp. 1575–1589. DOI: `10.2514/1.J054943`.

[11] Dieter Lasser. *Grundlagen der geometrischen Datenverarbeitung*. Springer-Verlag, 2013.

[12] Patrick Wegener and Stefan Keye. "CAD deformation for the consideration of aeroelastic effects". In: *33rd Congress of the International Council of the Aeronautical Sciences, ICAS 2022*. Vol. 3. 2022, pp. 2325–2333.